

Ge(001) surface reconstruction studied using a first-principles calculation and a Monte Carlo simulation

Yoshihide Yoshimoto

Department of Physics, Graduate School of Science, University of Tokyo, 7-3-1 Hongo, Bunkyo-ku, Tokyo 113-0033, Japan

Yoshimichi Nakamura

Venture Business Laboratory, Kyushu University, Hakozaki, Fukuoka 812-8581, Japan

Hiroshi Kawai

Department of Physics, Faculty of Science, Kyushu University, Ropponmatsu, Fukuoka 810-8560, Japan

Masaru Tsukada

Department of Physics, Graduate School of Science, University of Tokyo, 7-3-1 Hongo, Bunkyo-ku, Tokyo 113-0033, Japan

Masatoshi Nakayama

Department of Physics, Faculty of Science, Kyushu University, Ropponmatsu, Fukuoka 810-8560, Japan

(Received 23 April 1999)

The problem of the relative energetic stabilities of high-order reconstructions of the Ge(001) surface is revisited with more refined first-principles calculations. Deducing the parameters of the Ising model from this result, we perform Monte Carlo simulations of the phase transition of the asymmetric dimer directions. The Monte Carlo simulation reproduces fairly well the experimental transition temperature of an x-ray-diffraction experiment. The potential-energy curve of the dimer flip-flop motion in the $p(2\times 1)$ structure is determined. The obtained geometry of the $c(4\times 2)$ structure also agrees fairly well with the results of an x-ray diffraction experiment.

I. INTRODUCTION

The Ge(001) surface has reconstructed structures similar to those of the Si(001) surface. The neighboring surface atoms form dimers, and each dimer buckles in order to stabilize, resulting in asymmetric dimer structures. The buckled dimers line up along the $\langle 110 \rangle$ direction and form “dimer row” structures. There are several possible surface reconstruction structures characterized by the ordering of the dimer buckle directions: the $p(2\times 1)$ structure, the $p(2\times 2)$ structure, the $c(4\times 2)$ structure, etc.¹ The Ge(001) surface has a $p(2\times 1)$ structure at room temperature, which turns into a $c(4\times 2)$ structure when it is cooled below 200 K. This phase transition of the Ge(001) surface, as well as that of the Si(001) surface has been theoretically studied with the model of an Ising spin system by treating the buckled dimers as interacting spins.²⁻⁷

One reason why the dimer fluctuation dynamics on the surfaces of the Ge(001) and Si(001) have attracted so much interest is that these surfaces provide a simple ideal system to observe the fundamental processes of statistical mechanics, such as phase transitions and critical phenomena. In particular, they can be observed both in real space by the scanning tunneling microscope (STM) and in reciprocal space by x-ray diffraction, low-energy electron diffraction, etc. One of the remarkable aspects of these systems is that, from observation in real space, interesting behaviors of the dimer fluctuation statistics induced by nonperiodic structures, such as the defects and the steps, can be studied directly. This is an attractive point of these dimer systems compared with mag-

netic spin systems, where the spatial behavior of the spins has been observed only in reciprocal space.

Theoretical studies on the phase transition of the Ge(001) surface have often used statistical mechanics simulations such as the Monte Carlo method. To perform these simulations, model parameters of the Ising spin system which mimic the tilting directions of the dimers must be determined. The model parameters can be determined using first-principles calculations by comparing the relative total energies of a sufficient number of different reconstruction models such as $p(2\times 1)$, $p(2\times 2)$, $c(4\times 2)$, and $p(4\times 1)$ structures. The accuracy of a first-principles calculation itself can be evaluated by examining the reproducibility of the observed phase transition of this surface by a simulation based on model parameters determined using the first-principles calculation.

However, the absolute difference in the stabilization energies per dimer between the $p(2\times 2)$ and $c(4\times 2)$ structures, which determines the ground state of the reconstructed structures, is fairly small, estimated to be under 5 meV/dimer. The previous calculation⁸ was not able to determine this parameter.

The charge transfer between up-atom and down-atom dimer causes dipole interaction among dimers, and this interaction “prefers” $p(2\times 2)$.³ However, elastic interaction between dimers prefers $c(4\times 2)$ (see Fig. 1). Therefore we should treat both interactions simultaneously. Since first-principles calculations fully treat the electrostatic energy of the electron density and ions, they can determine the balance between the dipole interaction and elastic interaction.

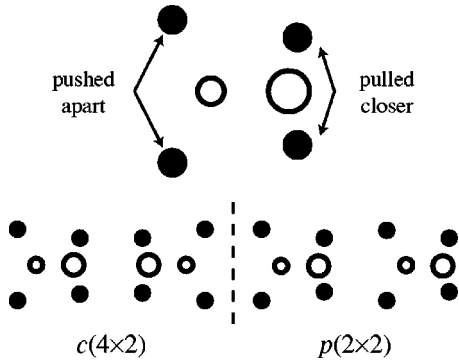


FIG. 1. Top: substrate relaxation around a dimer. Second-layer atoms under the up-atom dimer are pulled closer. Second-layer atoms under the down-atom dimer are pushed apart. Bottom: interaction of substrate relaxation between dimer rows. $c(4 \times 2)$ is preferable to $p(2 \times 2)$.

In the present work we attempt to reexamine this energy difference with a better precision insofar as possible by more accurate calculations than the one reported previously. Actually, the present calculation indicates that the most stable structure is the $c(4 \times 2)$, which agrees with the experimental fact.

Using the values of the parameters determined by the present first-principles results of the relative stability data, we perform a Monte Carlo simulation (MCS) for arrangements of asymmetric dimers on the Ge(001) surface. We shall see below that the coupling constants for the Ge(001) surface have nearly the same anisotropic character as those for the Si(001) surface.⁹ It will be shown that in thermal equilibrium, the statistical behavior of a defect-free Ge(001) surface is almost the same as that of a Si(001) surface. We shall see that the order-disorder phase transition occurs at about 315 K, which is nearly equal to the middle of the transient temperature region observed by an x-ray experiment.¹⁰

The dynamics of the dimer flip-flop motion can be observed by the STM. The theoretical simulation of this dynamics requires the potential surface of the dimer flip-flop motion. In the present study, the potential curve of the Ge dimer flip-flop motion in the $p(2 \times 1)$ structure is obtained. This potential surface should be parametrized by a multi-dimer orientation relation. However, due to the computational cost, we treat only the minimal case. The geometry of the $c(4 \times 2)$ structure of the present study agrees fairly well

TABLE I. Comparison between the Ceperley-Alder-type exchange correlation potential applied to the bulk Ge, and the Perdew-Wang 91 exchange correlation potential applied to the bulk Ge. The deviations from the experimental value are compared. a , B , and E_c are the lattice constant, the bulk modulus, and the cohesive energy, respectively.

	a	B	E_c
Ceperley-Alder	-0.2%	0.12%	15.0%
Perdew-Wang 91	1.2%	-13.1%	2.0%

with that obtained in an x-ray-diffraction experiment at 150 K.¹¹

II. METHOD OF FIRST-PRINCIPLES CALCULATION

The framework of our calculations is the density-functional theory.^{12,13} To select the exchange correlation potential, we compare the Ceperley-Alder-type^{14,15} and Perdew-Wang-91-type¹⁶ exchange correlation potentials. (“Perdew-Wang 91” is a gradient-corrected functional.) This comparison is based on the bulk Ge calculation shown in Table I. The Ceperley-Alder-type exchange correlation potential reproduces the experimental lattice constant and the experimental bulk modulus better. On the other hand, the Perdew-Wang-91-type potential reproduces the experimental cohesive energy better. As far as we know, the origin of this difference is not well known. However, this difference is empirically well known.¹⁷

We suppose that the subtle stability difference between the $p(2 \times 2)$ structure and the $c(4 \times 2)$ structure is governed mainly by the elasticity. Hence we select the Ceperley-Alder-type exchange-correlation potential^{14,15} for the present study. The core electrons of the Ge atoms are treated by the Troullier-Martins-type norm-conserving pseudopotential.¹⁸

The surfaces were simulated by the repeated slab model. To prevent the unphysical torsion of the slab, we used a calculated bulk lattice constant to construct the slab model, fixing the atom positions of the bottom layer. The calculated bulk lattice constant is 5.64865 Å. The slab was eight-atomic layers thick. The bottom of the slab was terminated by one virtual hydrogen atom layer. The vacuum region was eight-atomic layers thick for the comparison of the $c(4 \times 2)$ and $p(2 \times 2)$ structures, and four-atomic layers thick

TABLE II. Convergence checks. N_k is the total number of the sample k points in the first Brillouin zone. G_c^2 is the cutoff energy of the plane wave basis set in Ry. ΔE is the total energy difference per dimer in units of meV.

	$p(2 \times 1)$ -sym - $p(2 \times 1)$		$p(2 \times 1)$ - $p(2 \times 2)$	
	values	ΔE	values	ΔE
N_k	12, 24, 32	251.0, 293.7, 294.4	16, 32	86.7, 85.4
G_c	3.66, 4.0, 4.5, 5.0	294.4, 289.8, 290.7, 294.9	3.66, 4.0	86.7, 88.7
	$p(4 \times 1)$ - $p(2 \times 1)$		$p(2 \times 2)$ - $c(4 \times 2)$	
	values	ΔE	values	ΔE
N_k	8, 12, 16	31.8, 30.6, 29.8	8, 24, 32	1.1, 1.2, 1.3
G_c	3.66, 4.0, 4.5	29.8, 28.8, 29.8	4.0, 4.5, 5.0	1.2, 1.2, 1.2

TABLE III. Energetic stability per dimer (meV).

	$p(2\times 1)$ -sym	$p(4\times 1)$	$p(2\times 1)$	$p(2\times 2)$	$c(4\times 2)$
present	382.3	117.7	87.9	1.2	0
Ref. 8	—	101	66	-3	0
Ref. 21	290	—	50	—	0
Si: Ref. 9	260.5	117.6	90.6	1.2	0

for the other comparisons. For each comparison of the reconstructed structure, the supercell of the lateral direction was set to be the minimum cell which simultaneously contains the two compared structures.

We took the cutoff energy of the plane-wave basis set to be 13.4 Ry except in the comparison between the $c(4\times 2)$ and $p(2\times 2)$ structures, for which we took 16 Ry. The total numbers of the sampled k points for each comparison were 32, 16, 16, and 24 for $p(2\times 1)$ -sym vs $p(2\times 1)$, $p(2\times 2)$ vs $p(2\times 1)$, $p(4\times 1)$ vs $p(2\times 1)$, and $p(2\times 2)$ vs $c(4\times 2)$, respectively. The convergence checks of the cutoff energy and the total sampled k points are shown in Table II. Symmetry-restricted geometry optimizations were performed for all the atoms except those in the virtual hydrogen layer and the lowest Ge layer. The remaining force acting on the relaxed atoms in the optimized geometry was 3×10^{-4} Hartree/a.u. We used programs developed by Yamauchi *et al.*, the details of which are described in Ref. 19.

III. RELATIVE STABILITIES OF THE DIMER ARRANGEMENTS

The relative surface energies per dimer are summarized in Table III. Those for the Si(001) surface⁹ are also shown in this table. The $p(2\times 2)$ structure is higher by 1 meV than the $c(4\times 2)$ structure per dimer. The $p(2\times 1)$ -sym structure is higher than the $p(2\times 1)$ structure by 294 meV. For the Si case, this difference was reported as 169.9 meV in Ref. 9. Thus the barrier of the dimer flip-flop motion of Ge is significantly higher than that of Si.

The convergence error of the comparison between the $p(2\times 2)$ and $c(4\times 2)$ structures is estimated from Table II to be 0.1 meV/dimer. The influence of the thicknesses of the slab and vacuum on the energy difference per dimer between the $p(2\times 2)$ and $c(4\times 2)$ structures was also checked by test calculations. Changing the slab thickness from eight to 12 atomic layers thick resulted in an energy difference of less than 0.1 meV/dimer. Changing the vacuum thickness from four to eight atomic layers thick also resulted in an energy difference below 0.1 meV/dimer.

TABLE IV. Obtained $c(4\times 2)$ structure. The x and y coordinates refer to the $c(4\times 2)$ unit cell. The unit of the z coordinate is the bulk lattice constant. The labels of the atoms are shown in Fig. 3. The asterisks denote agreement with the assumed $c(4\times 2)$ symmetry.

	1	2	3	4	5	6	7	8
x	0.1874	0.3354	0.3692	0.25*	0.5*	0.0*	0.2513	0.5*
y	0.5*	0.5*	0.2670	0.25*	0.2511	0.5*	0.5*	0.5*
z	-0.0252	0.1230	-0.1607	-0.4435	-0.3946	-0.6492	-0.6893	-0.6541

Our results show that the $c(4\times 2)$ structure is more stable than the $p(2\times 2)$ structure. This result agrees with the experimental fact below 200 K, which shows the $c(4\times 2)$ structure as the most stable phase.^{11,20,10}

IV. GEOMETRY OF THE $c(4\times 2)$ STRUCTURE

The obtained geometry of the $c(4\times 2)$ structure shown in Table IV is compared with the geometry determined from an x-ray-diffraction experiment¹¹ in Table V. Since the bulk lattice constant of the present calculation and that of the above experiment are slightly different, we compare these two results in following manner: first, we compare them in the lattice coordinate; then we transform the obtained difference in the lattice coordinate to the difference in the Cartesian coordinate using the experimental lattice parameters.

The differences between the two results are small for the lateral direction. However, the differences for the vertical direction are somewhat larger. The accuracy of the experimental geometry for the vertical direction is worse than that of the lateral direction. The $c(4\times 2)$ symmetry also strictly restricts the lateral geometry. Therefore, it is not strange that the difference between the experiment and the numerical calculation is larger for the vertical direction. The obtained dimer tilting angle is 19° , which agrees well with the value $19^\circ \pm 1^\circ$ determined by the above experiment. Needels, Payne, and Joannopoulos obtained 14° as the dimer tilting angle.^{21,8} Spiess, Freeman, and Soukiassian obtained 15.4° as the dimer tilting angle.²²

V. MONTE CARLO SIMULATION OF THE PHASE TRANSITION

We introduce the model for the defect-free surface as follows. It is considered that only the arrangement of the asymmetric dimers is affected by a temperature up to several hundred K. Because the equilibrium angles of the four asymmetric structures take almost the same value, the tilting angles of each dimer are assumed to take only two values $\pm q_0$. The thermal flip-flop motion between the two angles is considered in the Monte Carlo simulation. The real system of dimers is thus projected onto the Ising spin model, in which the two degrees of freedom of an Ising spin correspond to the two possible tilting angles of an asymmetric dimer. We confirm that the Ising spin model which has been used in describing the arrangement of the dimers and the flip-flop motions on the Si(001) surface is also adequate for the Ge(001) surface. The model is described by the Ising spin Hamiltonian

TABLE V. $c(4 \times 2)$ structure difference from Table I of Ref. 11. Δx , Δy , and Δz denote the differences in each axis of the Cartesian coordinate. Δr denotes the distance between the atom position of the present work and that of the experiment referred to. The asterisks denote agreement with the assumed $c(4 \times 2)$ symmetry. The atom numbers 1–8 refer to Fig. 3

	1	2	3	4	5	6	7	8
Δx (10^{-2} Å)	-3.07	0.69	-3.87	0*	0*	0*	0.01	0*
Δy (10^{-2} Å)	0*	0*	-1.99	0*	0.56	0*	0*	0*
Δz (10^{-1} Å)	-0.001	0.0	-0.469	1.33	3.09	1.483	-0.042	1.137
Δr (10^{-1} Å)	0.307	0.069	0.640	1.33	3.09	1.483	0.042	1.137

$$H = V \sum_{i,j} S_{i,j} S_{i,j+1} + H \sum_{i,j} S_{i,j} S_{i+1,j} + D \sum_{i,j} S_{i,j} (S_{i-1,j+1} + S_{i+1,j+1}), \quad (5.1)$$

where $S_{i,j} = \pm 1$ corresponds to the angle $\pm q_0$ of the dimer at the site (i, j) defined in Fig. 2. The coupling constants are also illustrated in Fig. 2. The values of the parameters V , H , and D are determined by the energetic stability data obtained in Sec. IV. The details will be discussed in Sec. V A.

A. Model parameters of the Monte Carlo simulation

The values of the coupling constants V , H , and D for the Ge(001) surface are listed in Table VI together with those for the Si(001) surface (Fig. 3).⁹ It is remarkable that the values of V , H , and D for the Ge(001) surface are almost the same as those for the Si(001) surface. This is because the relative energy differences between the four asymmetric structures on each surface are almost the same. On both surfaces, V is much larger than the others, and its sign is positive. Therefore, the interaction along the dimer row strongly tends to set the orientations of the neighboring dimers along the dimer row “antiferromagnetic,” i.e., opposite to one another. This reflects the fact that the energies of the $p(2 \times 2)$ and $c(4 \times 2)$ structures are much lower than those of the other structures on both surfaces. When the asymmetric dimers in each dimer row are perfectly ordered antiferromagnetically, the interaction energy per dimer between the nearest-neighbor rows is given by $H - 2D$. As $H - 2D$ is a small but finite value with a positive sign (0.6 meV for both surfaces), the $c(4 \times 2)$ structure is energetically preferable to the $p(2 \times 2)$ structure on both surfaces.

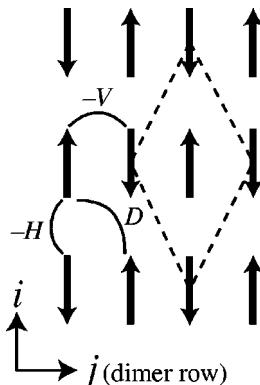


FIG. 2. Ising model of the $c(4 \times 2)$ structure.

B. Method of the Monte Carlo simulation

We perform a MCS on a system of 50 dimer rows \times 1000 dimers, employing periodic boundary conditions. The Metropolis algorithm is used to update the spin configuration. A set of trials updating the configurations of all the spins in the system is counted as “one Monte Carlo (MC) step.” At each temperature, the system reaches thermal equilibrium after 10^4 – 10^5 MC steps, and the succeeding 10^4 – (5×10^5) MC steps are employed to calculate thermodynamic averages. The latter MC steps are divided equally into ten segments, and sectional averages are calculated over each segment. Such data points are used to estimate the standard deviations which are shown as error bars in the figures presented below.

The long-range order parameter for the $c(4 \times 2)$ structure is defined as

$$\langle \Psi \rangle = \left\langle \sum_{i,j} (-1)^{i+j} S_{i,j} \right\rangle / N, \quad (5.2)$$

where N is the total number of spins ($N = 50 \times 1000$), and the brackets $\langle \dots \rangle$ denote the average over MC steps. The squared fluctuation of the long-range order parameter Ψ is defined as $\langle \chi \rangle = \langle (\Psi - \langle \Psi \rangle)^2 \rangle$. We calculate $\langle \Psi \rangle$ and $\langle \chi \rangle$ at each temperature.

C. Results of the Monte Carlo simulation and comparison with experiments

We show the results of a MCS for the defect-free Ge(001) surface. Figure 4 shows the temperature dependence of the long-range-order parameter $\langle \Psi \rangle$. $\langle \Psi \rangle$ fluctuates around zero at high temperature. When the temperature is lowered below around 315–310 K, the absolute value of $\langle \Psi \rangle$ increases rapidly to almost unity. A similar feature has also been observed for the defect-free Si(001) surface.^{9,5} At a lower temperature, the structure transforms into a single domain of the $c(4 \times 2)$ structure with asymmetric dimers. We show the temperature dependence of $\langle \chi \rangle$ in Fig. 5. It fluctuates around zero at higher temperatures. As the temperature is lowered

TABLE VI. Model parameters of the Si(001) and Ge(001) surfaces. V , H , and D are defined in Fig. 2.

	V	H	D
Si(001)	51.9	-6.6	-3.6
Ge(001)	51.1	-7.2	-3.9

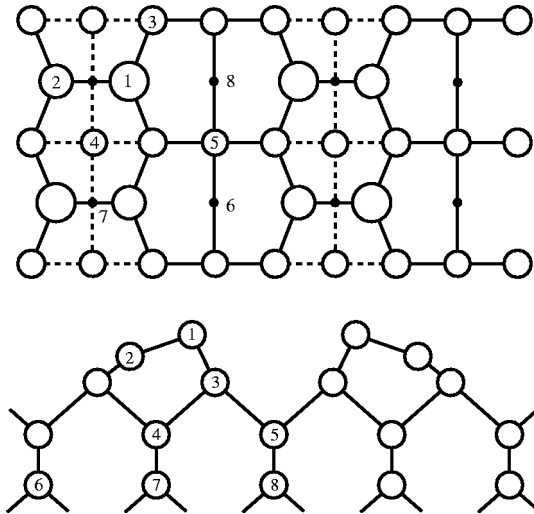


FIG. 3. Top: top view of the $c(4 \times 2)$ structure. Bottom: side view of the $c(4 \times 2)$ structure.

and approaches 315 K, $\langle \chi \rangle$ increases abruptly, and a sharp peak appears at 315 K. $\langle \chi \rangle$ becomes nearly zero again when the temperature is lowered below 310 K. From the present MCS, the transition temperature of the defect-free Ge(001) surface is estimated to be about 315 K. This is almost equal to the middle point of the broad transition region (250–350 K) observed by Lucas *et al.* in an x-ray-diffraction experiment.¹⁰ Therefore, we can conclude that the Ising model parameters determined by the first-principles calculations can reproduce an experimental phase transition temperature of the $c(4 \times 2) \leftrightarrow p(2 \times 2)$.

We note that the experimentally observed phase transition of the Ge(001) surface is not as sharp as that predicted by the present MCS for a defect-free system. It was shown in the experiment¹⁰ that the real surface consists of multidomains of the $c(4 \times 2)$ structure which are not fully ordered into a single domain. The domain sizes of the $c(4 \times 2)$ structure were estimated to be about 50 dimers \times 6 dimer rows at 170 K from the half-width at half-maximum of the quarter-order spot.¹⁰ This is much smaller than the $p(2 \times 1)$ domain sizes estimated from the half-order spots (about 250 dimers \times 125 dimer rows).¹⁰ Lucas *et al.* concluded that this is due to the pinning of the $c(4 \times 2)$ domains by defects or impurity atoms. If this is the case, we are unable to observe any universal critical behavior. As for the Si(001) surface, it has been clearly shown by MCS that a small number of type-C defects influence the formations of the local domains and

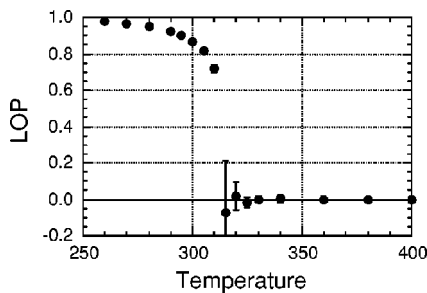


FIG. 4. Temperature dependence of the long-range order parameter.

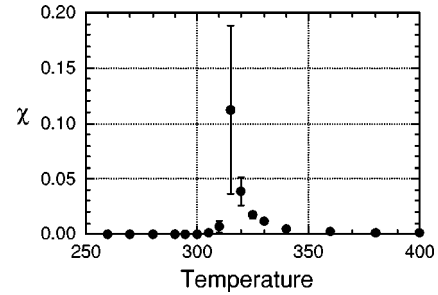


FIG. 5. Temperature dependence of the fluctuation χ .

modify the feature of the phase transition. The broad transition observed by LEED on the Si(001) surface has been well reproduced by the MCS.⁵ The type-C defect influences the ordering of the nearby dimers and plays the role of ‘‘phase shifter.’’²³ The type-C defects are typically seen in many STM images of the Si(001) surface, but not in those of the Ge(001) surface. It is considered that the $c(4 \times 2)$ domain structures on the Ge(001) surface are sensitive to some other defects. If such defects are identified by STM observations, we can more precisely analyze the order-disorder phase transition of the real Ge(001) surface by MCS, which treats the defects on the basis of the STM observations.

VI. DISCUSSIONS

We comment briefly on the dynamics of the Si(001) and Ge(001) surfaces. It is considered that the flip-flop motion between the two stable configurations of each dimer occurs via a symmetric dimer configuration. Therefore, the energy difference between the symmetric and asymmetric dimer ΔE_{s-a} concerns the time scale of the flip-flop motion. We see from Table III that ΔE_{s-a} of Ge(001) is larger by about 120 meV than that of Si(001). This implies that the transition rate between the two stable configurations of Ge(001) is much smaller than that of Si(001). On the other hand, the coupling constants V , H , and D , and the transition temperature region for Ge(001), are almost the same as those for Si(001). This means that the thermal equilibrium structures of both surfaces are almost the same at each temperature, but the time scale of the thermal fluctuations of the Ge(001) surface is much larger than that of the Si(001) surface. The lower the temperature the larger the difference becomes. It is expected that an extremely long observation time will be required to observe the thermal equilibrium Ge(001) surface at low temperature. In order to interpret the experimental data theoretically, the influence of surface defects and the scales of space and time of the observations should be taken into consideration. Such studies are now in progress.

As a first step, we calculated the total-energy curve of the Ge dimer flip-flop motion in the $p(2 \times 1)$ structure (the solid line in Fig. 6). The interpolation of the extreme points by a fourth-order polynomial is shown by the dashed line. The difference between the two curves in the figure shows that the interpolation of the extreme points by a fourth-order polynomial is not sufficiently small for a quantitative treatment of the dimer flip-flop motions. For example, the second-order derivative A at the minimum point in $10^{-3}[\text{eV}/\text{deg}^2]$ is 2.52 and 6.76 for the calculated curve and the interpolated curve, respectively. Since the pre-

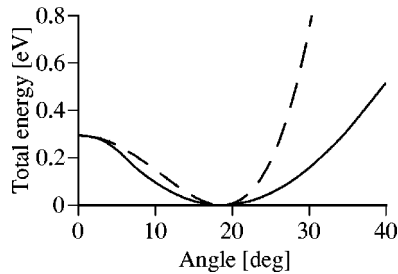


FIG. 6. Total-energy curve of the dimer tilting angle. The solid line denotes the present calculation. The dashed line denotes the interpolation of the extreme points by a fourth-order polynomial.

exponential factor of the thermal flip-flop probability is proportional to the square root of A , the interpolation is sufficient for a qualitative treatment. Within a parabolic approximation, the vibration energy around the minimum point is $\frac{1}{2}k_B T$, which is independent of A . These results will help future quantitative studies of the dynamics of the dimer motions.

VII. SUMMARY

The relative surface energies of the Ge(001) high-order reconstructions were determined by density-functional calcu-

lations. The most stable structure turned out to be the $c(4 \times 2)$ structure, which has a lower energy than the $p(2 \times 2)$ structure by 1.2 meV per dimer. The potential curve of the dimer flip-flop motion in the $p(2 \times 1)$ structure was also determined. The parameters of the Ising model for describing the arrangement of the dimer tilting directions were deduced from the relative surface energies. A Monte Carlo simulation based on the Ising model reproduced fairly well the phase transition temperature of the Ge(001) surface determined by an x-ray-diffraction experiment. The obtained $c(4 \times 2)$ structure reproduced fairly well the structure obtained by x-ray diffraction.

ACKNOWLEDGMENTS

This work was supported in part by a Grant-in-Aid from the Ministry of Education, Science, Sports and Culture of Japan, in part by the Core Research for Evolutional Science and Technology (CREST) of the Japan Science and Technology Corporation (JST), and in part by the JSPS Research for the Future Program in the Area of Atomic-Scale Surface and Interface Dynamics. The numerical calculations were partially performed by FACOM VPP 500/40 at the Supercomputer Center, Institute for the Solid State Physics, the University of Tokyo, and FACOM VPP 700/56 at the Computer Center of Kyushu University.

-
- ¹D. J. Chadi, Phys. Rev. Lett. **43**, 43 (1979).
²V. E. Zubkus, P. J. Kundrotas, S. N. Molotkov, V. V. Tatarskij, and E. E. Tornau, Surf. Sci. **243**, 295 (1991).
³H. J. W. Zandvliet, D. Terpstra, and A. van Silfhout, J. Phys. (Paris) **3**, 409 (1991).
⁴H. J. W. Zandvliet, W. J. Caspers, and A. van Silfhout, Solid State Commun. **78**, 455 (1991).
⁵Y. Nakamura, H. Kawai, and M. Nakayama, Phys. Rev. B **55**, 10 549 (1997).
⁶Y. Nakamura, H. Kawai, and M. Nakayama, Phys. Rev. B **52**, 8231 (1995).
⁷Y. Nakamura, H. Kawai, and M. Nakayama, Surf. Sci. **357–358**, 500 (1995).
⁸M. Needels, M. C. Payne, and J. D. Joannopoulos, Phys. Rev. B **38**, 5543 (1988).
⁹K. Inoue, Y. Morikawa, K. Terakura, and M. Nakayama, Phys. Rev. B **49**, 14 774 (1994).
¹⁰C. A. Lucas, C. S. Dower, D. F. McMorrow, G. C. L. Wong, F. J. Lamelas, and P. H. Fuoss, Phys. Rev. B **47**, 10 375 (1993).
¹¹S. Ferrer, X. Torrelles, V. H. Etgens, H. A. van der Vegt, and P. Fajardo, Phys. Rev. Lett. **75**, 1771 (1995).
¹²P. Hohenberg and W. Kohn, Phys. Rev. **136**, B864 (1964).
¹³W. Kohn and L. J. Sham, Phys. Rev. **140**, A1133 (1965).
¹⁴D. M. Ceperley and B. J. Alder, Phys. Rev. Lett. **45**, 566 (1980).
¹⁵J. P. Perdew and A. Zunger, Phys. Rev. B **23**, 5048 (1981).
¹⁶J. P. Perdew, J. A. Chevary, S. H. Vosko, K. A. Jackson, M. R. Pederson, D. J. Singh, and C. Fiolhais, Phys. Rev. B **46**, 6671 (1992).
¹⁷Y.-M. Juan and E. Kaxiras, Phys. Rev. B **48**, 14 944 (1993).
¹⁸N. Troullier and J. L. Martins, Phys. Rev. B **43**, 1993 (1991).
¹⁹J. Yamauchi, M. Tsukada, S. Watanabe, and O. Sugino, Phys. Rev. B **54**, 5586 (1996).
²⁰S. D. Kevan, Phys. Rev. B **32**, 2344 (1985).
²¹M. Needels, M. C. Payne, and J. D. Joannopoulos, Phys. Rev. Lett. **58**, 1765 (1987).
²²L. Spiess, A. J. Freeman, and P. Soukiassian, Phys. Rev. B **50**, 2249 (1994).
²³H. Tochiohara, T. Amakusa, and M. Twatsuki, Phys. Rev. B **50**, 12 262 (1994).